38p

S 54330 40B

NASA TM X-26

~~N62-71850~~

N63-12976
Code-1

NASA TM X-26

TECHNICAL MEMORANDUM
X-26

DESIGN GUIDE FOR PITCH-UP EVALUATION AND INVESTIGATION AT HIGH SUBSONIC SPEEDS OF POSSIBLE LIMITATIONS DUE TO WING-ASPECT-RATIO VARIATIONS

By Kenneth P. Spreemann

Langley Research Center
Langley Field, Va.

Declassified July 11, 1961

NATIONAL AERONAUTICS AND SPACE ADMINISTRATION
WASHINGTON August 1959

1F

NATIONAL AERONAUTICS AND SPACE ADMINISTRATION

TECHNICAL MEMORANDUM X-26

DESIGN GUIDE FOR PITCH-UP EVALUATION AND INVESTIGATION AT HIGH SUBSONIC SPEEDS OF POSSIBLE LIMITATIONS DUE TO WING-ASPECT-RATIO VARIATIONS

By Kenneth P. Spreemann

SUMMARY

A design guide is suggested as a basis for indicating combinations of airplane design variables for which the possibilities of pitch-up are minimized for tail-behind-wing and tailless airplane configurations. The guide specifies wing plan forms that would be expected to show increased tail-off stability with increasing lift and plan forms that show decreased tail-off stability with increasing lift. Boundaries indicating tail-behind-wing positions that should be considered along with given tail-off characteristics also are suggested.

An investigation of one possible limitation of the guide with respect to the effects of wing-aspect-ratio variations on the contribution to stability of a high tail has been made in the Langley high-speed 7- by 10-foot tunnel through a Mach number range from 0.60 to 0.92. The measured pitching-moment characteristics were found to be consistent with those of the design guide through the lift range for aspect ratios from 3.0 to 2.0. However, a configuration with an aspect ratio of 1.55 failed to provide the predicted pitch-up warning characterized by sharply increasing stability at the high lifts following the initial stall before pitching up. Thus, it appears that the design guide presented herein might not be applicable when the wing aspect ratio is lower than about 2.0.

INTRODUCTION

The phenomenon of longitudinal instability at high lift and the associated probability of an undesirable divergence, commonly referred to as pitch-up, have presented a complex problem to designers of high-speed airplanes for many years. Generally, the designer is faced with the following considerations: (1) try to arrive at an aerodynamic layout for which pitch-up is unlikely or, at least, not severe, (2) evaluate the possible severity of the motion by means of a dynamic analysis of the type outlined in reference 1, and (3) if undesirable behavior is associated with the particular design that appears to be the best compromise of all requirements, provide sufficient artificial stabilization to minimize pitch-up as a problem.

The present paper deals primarily with the first of these considerations. The objectives are twofold: first, to present a design guide (based on a considerable background of experience) to indicate combinations of design variables for which the possibilities of pitch-up are minimized; and second, to investigate one possible limitation of the guide with respect to the effect of wing-aspect-ratio variations on the tail contribution. The design guide presented is limited in applicability because the background information considered is predominately from investigations concerned with fighter airplanes having wings with rather low aspect ratios and being of the tailless or tail-behind-wing types. The results, therefore, have their most direct application to such configurations having aspect ratios from about 2 to 5.

L
4
2
7

COEFFICIENTS AND SYMBOLS

Figure 1 shows the stability system of axes employed for data presentation with arrows indicating positive directions of forces, moments, and angles. The coefficients and symbols used are defined as follows:

C_L	lift coefficient, Lift/qS
C_D	drag coefficient, Drag/qS
C_m	pitching-moment coefficient, Pitching moment/$qS\bar{c}$
$C_{L,max}$	maximum lift coefficient
q	dynamic pressure, $\rho V^2/2$, lb/sq ft
ρ	mass density of air, slugs/cu ft
V	free-stream velocity, ft/sec
M	Mach number

S	surface area, sq ft
b	span, ft
c	local chord parallel to plane of symmetry, ft
$\bar{c}$	mean aerodynamic chord, $\frac{2}{S}\int_0^{b/2} c^2 dy$, ft
$\bar{c}_V$	mean aerodynamic chord of vertical tail, ft
l	tail length (distance between quarter-chord points of wing and horizontal-tail mean aerodynamic chords), ft
x	afterbody distance along body axis, ft
y	spanwise distance from plane of symmetry on wing, ft
z	tail position (height of tail above wing chord plane), ft
D	diameter, in.
r	radius, in.
A	aspect ratio, b^2/S
Λ	angle of sweep, deg
$\Lambda_{c/4}$	angle of sweep of lifting-surface quarter chord, deg
λ	taper ratio, Tip chord/Root chord
R	Reynolds number
α	angle of attack, deg
i	angle of incidence of fixed surface, deg
ϵ	downwash angle induced by wing-fuselage combination, deg

$$\epsilon_{C_L} = \frac{\partial \epsilon}{\partial C_L}$$

L
4
2
7

Subscripts:

max maximum

t horizontal tail

b model base

Abbreviations:

c.g. center-of-gravity location

L427

W wing

F fuselage

V vertical tail

H horizontal tail

DESIGN GUIDE FOR PITCH-UP EVALUATION

Wing and Wing-Fuselage Combinations

The problem of pitching-moment nonlinearity at high lift coefficients for wings and wing-fuselage combinations has been studied by numerous investigators. For the most part, correlations have been made in terms of the wing sweep angle and aspect ratio, with varying degrees of consideration given to the taper ratio. Wing-thickness effects normally have been neglected, although the studies usually have been limited to wings that are thin enough to avoid any significant moment breaks due to thickness within the Mach number range investigated. Effects of camber, twist, cranked plan forms, or any of the localized wing modifications, such as fences, leading-edge extensions, or notches, have not been treated in any generalized sense. Such devices, though frequently very effective in improving pitching-moment linearity, normally must be tailored to the specific wing in question. A considerable number of such studies have been reported. It also has been commonly assumed that results on wings alone or on wing-fuselage combinations may be used interchangeably, insofar as pitching-moment linearity is concerned. This appears to be justified for configurations having the proportions of manned aircraft in the subsonic and transonic speed ranges.

An investigation (ref. 2) in which some rather extreme changes in forebody geometry were made showed little effect on the nature of the moment breaks or on the angle of attack at which they occurred, but it indicated significant effects at angles of attack well beyond the initial moment breaks. For missile configurations, having large bodies in comparison with the size of the wings, the fuselage characteristics may be predominant and, consequently, cannot be ignored. Some evidence exists which indicates that a tendency toward a similar situation may apply to supersonic-airplane configurations. (See ref. 3.)

Several of the correlation boundaries that have been presented in the literature are summarized in figure 2. All are given in terms of coordinates of aspect ratio and sweep angle and in each instance the area above and to the right of the curve is characterized by decreased stability at the higher lift coefficients; whereas, the area below and to the left of the curve is characterized by increased stability at high lift. The range of data considered and the specific interpretation of each of the boundaries differ, however, as will be explained in the following paragraphs.

The oldest and most widely known of the boundaries is that labeled "1" in figure 2 and given by Shortal and Maggin (ref. 4). Though based on only a limited amount of low-speed test data, it has served as a useful design criterion for many years. This boundary considers moment changes in the vicinity of maximum lift, without regard to slope changes in the intermediate lift range. Information obtained at a later date on more highly tapered wings showed that when attention was still confined to nonlinearities near maximum lift, a rather large effect of taper was indicated. Consequently, Furlong and McHugh (ref. 5) proposed an empirical expression for low-speed boundaries in which the taper ratio entered as a variable. The boundary evolved for $\lambda = 0$ is indicated in figure 2 as the curve labeled "2." No significant change from the Shortal-Maggin boundary was indicated for untapered wings.

As wind-tunnel experience increased in the high subsonic and transonic speed range, the phenomenon of shock stall and the associated center-of-pressure changes were seen to impose limitations on the applicability of the boundaries derived from low-speed data. Studies made by Weil and Gray of the limited amount of high-speed data available in 1953 led to the proposal of a tentative boundary applicable to transonic speeds (ref. 6). This boundary, labeled "3" in figure 2, showed that in order to avoid stability reductions at the higher speeds, values of aspect ratio and sweep angle considerably lower than those indicated by the low-speed boundaries were required. The results available were insufficient to establish an effect of taper ratio, and the true significance of the boundary as to the lift coefficients at which the moment changes occurred was not clearly defined. Weil and Gray (ref. 6) pointed out the relation of their boundary to tail position. That is, wings represented by combinations of aspect ratio and sweep angle in the area above and to the right of the boundary probably could be used with a very low tail; whereas a very high tail may be feasible if wings represented by the area below and to the left of the boundary are used.

This viewpoint inspired a systematic program aimed at defining the tail-off boundary more precisely and indicating fairly specific areas where the tail might be located. The resulting tail-off boundary as proposed by Few and Fournier in reference 7 is the curve labeled "4" in figure 2. In this case, extensive transonic data were considered, and the boundary was established to separate plan forms showing at any positive lift coefficient below $C_{L,max}$ a value of $\partial C_m/\partial C_L$ less negative than that at $C_L = 0$ (area above boundary) from plan forms showing a value of $\partial C_m/\partial C_L$ more negative at positive lift than at $C_L = 0$. A boundary defined in this manner was considered to bear a more useful relation to the requirements for tail position than a boundary determined by moment changes only near $C_{L,max}$. The boundary obtained is almost identical to that proposed in reference 6 by Weil and Gray; however, the additional restriction that application should be limited to highly tapered wings (λ from 0 to 0.4) has been imposed. Wings having higher values of λ were found to exhibit rather erratic nonlinearities at high lift and, therefore, were not well adapted to correlation on a simplified basis.

L427

Tail Position

The curve labeled "4" in figure 2 provides the basis for wing selection in the design chart given in figure 3(a). This is the boundary proposed by Few and Fournier in reference 7, which has been adopted for the present correlation since the configuration limitations imposed in reference 7 are adaptable to the bulk of data available on the effects of wing-aspect-ratio variations on the tail contribution to stability, with which the present investigation is partly concerned. This boundary has been extended to lower aspect ratios than those presented in reference 7, with the extension based on data of other investigations such as references 8 and 9. Since the linearity of the horizontal-tail pitching-moment contribution associated with any given design is governed by a large number of factors, any attempt to simplify the problem of tail-position selection to a simple chart procedure may seem unjustified. It is also true, however, that sufficient knowledge of all contributing factors in combination, which would be necessary in a rigorous approach to the problem, is not likely to be attained. The provision of a simple design guide, with a reasonable appreciation of its meaning and limitations, therefore, should serve a useful purpose. In the various attempts that have been made to establish boundaries for tail position, little consideration has been given to fuselage geometry. As has been noted with regard to tail-off characteristics, the origin of nonlinearities in the tail contribution appears to be determined primarily by the wing geometry and tail position, although at higher angles of attack fuselage forebody geometry seemingly plays an important part in the magnitude of the deviations from pitching-moment linearity (ref. 2). It should be noted that for some unusual cases (ref. 10) the effect of the fuselage afterbody may be of primary importance even at moderate angles of attack.

Several of the significant boundaries relative to tail positions and some notes on the significance of the areas between the boundaries are given in figure 3(b). The coordinates are tail length and tail position relative to the wing quarter-chord location. A boundary approximately in the location indicated by the curve labeled "1" was first given by Jaquet in reference 9 to separate regions where the increment in $\partial C_m/\partial C_L$ through the lift range of a tail behind a 60° delta wing varied by more then $0.05\bar{c}$ (above boundary) from regions where the increment varied by less than $0.05\bar{c}$ (below boundary). Only low-speed results were considered, and tail length was limited to about two mean-aerodynamic-chord lengths behind the center of gravity. Later, Mitchell (ref. 11) showed that essentially the same boundary (a line inclined 10° above the chord plane) could be interpreted as separating tail positions for which the downwash slope $d\epsilon/d\alpha$ becomes more positive with increasing lift (above boundary) from regions where $d\epsilon/d\alpha$ becomes less positive with increasing lift (below boundary). Mitchell's data in reference 11 included several wing plan forms, some results through transonic speeds, and extended back about four mean-aerodynamic-chord lengths behind the center of gravity. Subsequent transonic data (refs. 12, 13, and 14) revealed, however, that it was safest to apply this boundary only within the subcritical speed range, since downwash changes associated with shock stall are at times significant within the region immediately below the 10° line (curve labeled "1" in figure 3(b)). For airplanes intended to traverse the transonic speed range it is considered that tail positions below a boundary that is slightly below the wing chord plane (curve 2) are necessary in order to avoid significant destabilizing downwash changes.

In reference 9, Jaquet indicated that a high boundary might be desirable so that tail positions above the boundary would not encounter a destabilizing downwash variation within the normal operational range of flight lift coefficients (below the stall). The curve labeled "3" in figure 3(b) is a boundary representing this general viewpoint, which was arrived at after consideration of a very large amount of wind-tunnel data, both published and unpublished. The interpretation of this boundary in terms of design applications warrants especially careful consideration and will be dealt with in more detail in the next section.

Use of Design-Guide Chart for Complete Airplane Configurations

Although the tail-off stability boundary given in figure 3(a) already has been discussed, a somewhat more specific interpretation is warranted. Wings having combinations of aspect ratio and sweepback defined by the region above the boundary (region I) would be expected to exhibit local moment slopes $\partial C_m/\partial C_L$ less stable somewhere below $C_{L,max}$ than the slope through $C_L = 0$; whereas, within region II the local slopes within the positive lift range will generally be more stable than at $C_L = 0$. Therefore, when a tailless airplane is considered, wings on or slightly below the boundary would seem appropriate if losses in stability are to be avoided. Wings in region I normally should be considered only in combination with a tail position that provides increased stability with increasing lift, that is, region D in figure 3(b) if the airplane is intended to operate through transonic speeds, or either region C or D if operation is limited below the critical Mach number. Based on past experience it should be recognized that when it is desired to use a wing represented by a point considerably above the wing-fuselage stability boundary, a correspondingly large stabilizing effect of the tail should be provided at high angles of attack. Thus, it may be desirable to locate the tail a substantial distance below the appropriate boundary given in figure 3, and perhaps some additional means of reducing or avoiding pitching-moment nonlinearity may have to be provided. No attempt has been made herein to establish a means for matching the wing and tail nonlinearities properly in order to obtain a specific desired result for combinations employing wings displaced appreciably from the boundary.

The tail-position boundary labeled "3" in figure 3(b) is intended to define the minimum tail position required in order to delay the occurrence of severe increases in downwash (and the associated loss in tail contribution to stability) until the effective wing $C_{L,max}$ or first major break in the lift curve has been passed. The use of wings defined by region II in figure 3(a), in combination with the high tail position, normally will result in avoiding significant losses in stability of the configuration until the lift break has been passed. When this condition is fulfilled, a fairly definite stall warning in the form of buffet or a momentary increase in stability can be expected to precede pitch-up. The eventual occurrence of pitch-up is almost a certainty unless some additional unique stabilizing feature is employed. Alleviation and even elimination of the instability beyond the stall have been accomplished by use of auxiliary horizontal surfaces low on the fuselage afterbody (refs. 15 and 16) or as a consequence of the extended afterbody of a flying-boat hull (ref. 17).

L
4
2
7

The remarks that have been made relative to designs with tails in region (A) should perhaps be limited to the Mach number range within which no strong shock-wave interference between the wing and the tail exists. Interference from the wing trailing-edge shock wave has not seemed troublesome; however, reference 18 has shown that some undesirably large stability changes can result from interference of a strong leading-edge compression wave with a high horizontal tail.

For airplanes required to operate through a transonic speed range, the use of tails at intermediate positions (region (B) of figure 3(b)) will normally be associated with some degree of pitch-up, with little or no warning, regardless of the wing plan form. Experience has indicated, however, that the severity of the instability varies considerably for different configurations and cannot be readily anticipated. (See refs. 19 and 20.)

PRELIMINARY REMARKS ON INVESTIGATION OF EFFECTS OF LOW-ASPECT-RATIO WING

The preceding discussion has covered the use and interpretation of the design guide. Many limitations are recognized, and the following sections of this paper present the results of a wind-tunnel investigation of one geometric variable in which the background information is considered to be weak. The problem concerns the range of wing aspect ratios for which the upper tail-position boundary (curve (3) of fig. 3(b)) retains the significance that has been described.

In addition to the fact that the degree of wing-fuselage pitching-moment nonlinearity is dependent upon aspect ratio, there are several reasons why aspect-ratio limitations might be expected. For example, since aspect ratio has a large effect on the variation of the wing lift with angle of attack, the tail position relative to the wing wake for a given lift coefficient will be dependent upon aspect ratio. This might be especially important for tails located in the high position which are apt to be entering the wake near the stall. Also, configurations utilizing low-aspect-ratio wings very often have high values of the ratio of tail span to wing span which could appreciably alter the downwash characteristics. In order to determine the degree to which these various effects might alter the significance of the upper tail-position boundary, wind-tunnel tests were made on a high-tail configuration with the wing progressively clipped to provide lower aspect ratios and lower ratios of wing span to tail span. Although only the stability characteristics will be discussed in detail, the lift and drag data will be presented for the sake of completeness.

L
4
2
7

MODEL, APPARATUS, AND TESTS

A three-view drawing of the complete model showing the general arrangement and some of the pertinent dimensions of the aspect-ratio-3.0 configuration is presented in figure 4(a). Shown in figure 4(b) are the plan forms and dimensions of the wings having an aspect ratio of 1.55, 2.0, and 2.5 employed in this investigation. Details of the fuselage are presented in figure 5. A detailed description of the complete model is contained in reference 21. The model was tested on the sting-type support system shown in figure 6, and a strain-gage balance mounted inside the fuselage was used to measure the forces and moments on the model.

The investigation was made in the Langley high-speed 7- by 10-foot tunnel. Lift, drag, and pitching moment were measured through a Mach number range from 0.60 to 0.92 and an angle-of-attack range from about -2° to 24°. The variation of mean test Reynolds number with Mach number based on the mean aerodynamic chord of each wing is shown in figure 7.

Blockage corrections were determined by the method of reference 22 and were applied to the Mach numbers and dynamic pressures. Jet-boundary corrections, applied to the angle of attack and drag, were calculated by the method of reference 23. The jet-boundary corrections to pitching moment were considered negligible and were not applied to the data. Corrections to the drag coefficients for buoyancy due to longitudinal pressure gradients were about 0.0016 to 0.0017. These corrections were not applied to the data. Past experience had indicated that tare values would be small and, therefore, no tare corrections were applied to the data.

The angle of attack has been corrected for deflection of the sting support system under load. No attempt has been made to correct the data for aeroelastic distortion of the model. The drag results have not been corrected to the condition of free-stream static pressure at the fuselage base. This drag correction (base pressure drag coefficient $C_{D,b}$) is presented in figure 8. The corrected model drag data may be obtained by adding the base pressure drag coefficient to the drag determined from the strain-gage-balance measurements.

TEST RESULTS

The basic aerodynamic data of the various configurations are presented in figures 9 to 12 without horizontal tail and with a horizontal tail at two deflections (0° and -3°). In part (b) of figures 9 to 12 the fuselage-alone pitching moments are also presented. Shown in figure 13 is a direct comparison of the longitudinal aerodynamic characteristics of all four configurations with $i_t = 0^{\circ}$.

The stability parameters $\partial C_L/\partial\alpha$ and $\partial C_m/\partial C_L$ of the configurations presented in figure 14 were taken from figure 13. The slopes presented in this figure were measured between lift coefficients from 0 to about 0.3. Figure 15 shows the relation of the test configurations to the design guide boundaries of figure 3.

Stability in Low-Lift Range

Before discussing the results in relation to the design guide, a few remarks with regard to the effects of the aspect-ratio changes on the low-lift static stability might be of interest. In figure 14 the variation of the static-stability parameter $\partial C_m/\partial C_L$ and the lift-curve slope $\partial C_L/\partial\alpha$ are presented as a function of Mach number for the various aspect ratios. Figure 14(a) presents the results for the horizontal-tail-off configuration, and figure 14(b) presents those for the horizontal-tail-on configuration ($i_t = 0^{\circ}$). Of particular interest is the fact that, although reducing the aspect ratio from 3.0 to 1.55 resulted in a large destabilizing shift in the aerodynamic center for the tail-off configuration, it had little effect on the tail-on configuration. This, of course, indicates a large increase in the tail contribution to stability with decreasing aspect ratio. An analysis of the data showed that this could be accounted for by the wing lift-curve-slope decrease (which for a given lift coefficient places the tail at a higher geometric angle of attack) and by the fact that ϵ_{C_L} did not increase with decreasing aspect ratio. The reason that ϵ_{C_L} did not increase with decreasing aspect ratio is probably associated with the fact that with the tail in the high position the increase in the resultant induced velocity due to the inboard movement of the wingtip vortex relative to the tail is mostly a sidewash component with respect to the horizontal tail and, thus, less of the resultant is converted to downwash on the tail.

Aspect-Ratio Limitations to Design Guide

As previously pointed out the relation of the test configurations to the design guide of figure 3 is given in figure 15. As shown in figure 15(a) the aspect-ratio-3.0 wing that was swept 37° is above and to the right of the boundary indicating reductions in stability in the high lift range. From the basic moment data of the aspect-ratio-3.0 configuration (fig. 9(a)), reduced stability at the higher lifts were indicated with the tail off. Following the initial stall there was a large increase in stability before the occurrence of a sharp reduction in stability. Addition of the tail does not greatly alter the departures from the stability in the low lift range of the tail-off condition; however, a sharp pitch-up occurs following the initial stall and subsequent increase in the negative pitching moment.

L
4
2
7

In figure 15(a) it is seen that the aspect ratios of 2.5 to 1.55 are below and to the left of the boundary indicating increasing stability at the high lifts. With aspect ratios of 2.5 and 2.0 the tail-off pitching-moment curves became increasingly stable up to the usual large increase in stability in the stall region before encountering a pronounced unstable trend. (See figs. 10(a) and 11(a).) The progressive increases in stability in the medium and high lift range with the tail-off configuration were reduced to such an extent with the addition of the tail that very desirable linear variations in the pitching-moment curves were provided up to the stall and in the greatly increased stability region before pitching up.

The aspect-ratio-1.55 configuration furnished pitch characteristics in the medium lift range that were similar to those of configurations having aspect ratios of 2.5 and 2.0. However, with the tail on, in the high lift range the usual pitch-up warning in the form of a sharp increase in stability before pitching up did not appear. (See fig. 12(a).) Since the tail-off configuration did not evidence a pitch-up trend as pronounced at the highest lifts as that of the higher aspect-ratio configurations, it appears that the usual wing stall was delayed beyond the pitch-up caused by the tail entering the wing wake. Thus, it would seem that application of the boundaries established in figure 3(b) will not be satisfactory below an aspect ratio of about 2.0, even though the aspect-ratio-1.55 configuration is below and to the left of the boundary of figure 3(a) and near the boundary of figure 3(b); this result signifies increasing stability at high lifts and a tail position compatible with the wing-fuselage combination.

It may also be seen that, in general, there were significant reductions in pitch-up warning when the tail was added to the wing-body configuration since the large increases in stability before pitching up with the tail off were markedly reduced with addition of the tail regardless of the aspect ratio.

CONCLUDING REMARKS

A design guide has been suggested as a basis for indicating combinations of design variables for which the possibilties of pitch-up are minimized for tail-behind-wing and tailless airplane configurations. The guide specifies wing plan forms that would be expected to show increased tail-off stability with increasing lift and plan forms that show decreased tail-off stability with increasing lift. Boundaries indicating tail-behind-wing positions that should be considered along with given tail-off characteristics also are suggested.

An investigation of one possible limitation of the guide with respect to the effects of wing-aspect-ratio variations on a high-tail contribution to the stability has been made in the Langley high-speed 7- by 10-foot tunnel. The measured pitching-moment characteristics were found to be consistent with those of the design guide through the lift range for aspect ratios from 3.0 to 2.0. However, an aspect-ratio-1.55 configuration did not provide the predicted pitch-up warning characterized by sharply increasing stability at the high lifts following the initial stall before pitching up. Thus, it appears that the design guide presented herein might not be applicable when the wing aspect ratio is lower than about 2.0.

Langley Research Center,
National Aeronautics and Space Administration,
Langley Field, Va., March 26, 1959.

REFERENCES

1. Campbell, George S., and Weil, Joseph: The Interpretation of Nonlinear Pitching Moments in Relation to the Pitch-Up Problem. NACA RM L53I02, 1953.

2. Goodson, Kenneth W.: Effect of Nose Length, Fuselage Length, and Nose Fineness Ratio on the Longitudinal Aerodynamic Characteristics of Two Complete Models at High Subsonic Speeds. NASA MEMO 10-10-58L, 1958.

3. Nielsen, Jack N.: The Effects of Body Vortices and the Wing Shock-Expansion Field on the Pitch-Up Characteristics of Supersonic Airplanes. NACA RM A57L23, 1958.

4. Shortal, Joseph A., and Maggin, Bernard: Effect of Sweepback and Aspect Ratio on Longitudinal Stability Characteristics of Wings at Low Speeds. NACA TN 1093, 1946.

5. Furlong, G. Chester, and McHugh, James G.: A Summary and Analysis of the Low-Speed Longitudinal Characteristics of Swept Wings at High Reynolds Number. NACA Rep. 1339, 1957. (Supersedes NACA RM L52D16.)

6. Weil, Joseph, and Gray, W. H.: Recent Design Studies Directed Toward Elimination of Pitch-Up. NACA RM L53I23c, 1953.

7. Few, Albert G., Jr., and Fournier, Paul G.: Wind-Tunnel Investigation of the Aerodynamic Characteristics of a Series of Swept, Highly Tapered, Thin Wings at Transonic Speeds - Transonic-Bump Method. NACA RM L56I24, 1956.

8. Spreemann, Kenneth P.: Low-Speed Investigation of the Effects of Wing Dihedral Angle and Fin Length on the Static Stability Characteristics of a Model Having an 82° Delta Wing. NACA RM L55L30a, 1956.

9. Jaquet, Byron M.: Effects of Horizontal-Tail Position, Area, and Aspect Ratio on Low-Speed Static Longitudinal Stability and Control Characteristics of a 60° Triangular-Wing Model Having Various Triangular-All-Movable Horizontal Tails. NACA RM L51I06, 1951.

10. McKee, John W., and Riebe, John M.: An Investigation of a 0.16-Scale Model of the Douglas X-3 Airplane To Determine Means of Improving the Low-Speed Longitudinal Stability and Control Characteristics. NACA RM L52H01, 1952.

11. Mitchell, Jesse L.: The Static and Dynamic Longitudinal Stability Characteristics of Some Supersonic Aircraft Configurations. NACA RM L52A10a, 1952.

12. Morrison, William D., Jr., and Alford, William J., Jr.: Effects of Horizontal-Tail Position and a Wing Leading-Edge Modification Consisting of a Full-Span Flap and a Partial-Span Chord-Extension on the Aerodynamic Characteristics in Pitch at High Subsonic Speeds of a Model With a 45° Sweptback Wing. NACA TN 3952, 1957. (Supersedes NACA RM L53E06.)

13. Bielat, Ralph P., and Campbell, George S.: A Transonic Wind-Tunnel Investigation of the Longitudinal Stability and Control Characteristics of a 0.09-Scale Model of the Bell X-5 Research Airplane and Comparison With Flight. NACA RM L53H18, 1953.

14. Runckel, Jack F., and Schmeer, James W.: The Aerodynamic Characteristics at Transonic Speeds of a Model With a 45° Sweptback Wing, Including the Effect of Leading-Edge Slats and a Low Horizontal Tail. NACA RM L53J08, 1954.

15. Sleeman, William C., Jr.: Investigation at High Subsonic Speeds of the Use of Low Auxiliary Tail Surfaces Having Dihedral To Improve the Longitudinal and Directional Stability of a T-Tail Model at High Lift. NACA RM L57I24, 1957.

16. Goodson, Kenneth W.: Static Longitudinal Characteristics at High Subsonic Speeds of a Complete Airplane Model With a Highly Tapered Wing Having the 0.80 Chord Line Unswept and With Several Tail Configurations. NACA RM L56J03, 1957.

17. Petynia, William W., Croom, Delwin R., and Davenport, Edwin E.: Low-Speed Aerodynamic and Hydrodynamic Characteristics of a Proposed Supersonic Multijet Water-Based Hydro-Ski Aircraft With Upward-Rotating Engines. NASA MEMO 10-13-58L, 1958.

18. Jaquet, Byron M., and Fournier, Roger H.: Effects of Wing Sweep, Horizontal-Tail Configuration, and a Ventral Fin on Static Stability Characteristics of a Model With a Wing of Aspect Ratio 3 at Mach Numbers From 2.29 to 4.65. NACA RM L58E06, 1958.

19. Goodson, Kenneth W., and Becht, Robert E.: Wind-Tunnel Investigation at High Subsonic Speeds of the Static Longitudinal Stability Charteristics of a Complete Model Having Cropped-Delta, Swept, and Unswept Wings and Several Horizontal-Tail Heights. NACA RM L54H12, 1954.

20. Hieser, Gerald, Henderson, James H., and Swihart, John M.: Transonic Aerodynamic and Loads Characteristics of a 4-Percent-Thick Unswept-Wing—Fuselage Combination. NACA RM L54B24, 1954.

21. Polhamus, Edward C., and Spreemann, Kenneth P.: Effect at High Subsonic Speeds of Fuselage Forebody Strakes on the Static Stability and Vertical-Tail-Load Characteristics of a Complete Model Having a Delta Wing. NACA RM L57K15a, 1958.

22. Herriot, John G.: Blockage Corrections for Three-Dimensional-Flow Closed-Throat Wind Tunnels, With Consideration of the Effect of Compressibility. NACA Rep. 995, 1950. (Supersedes NACA RM A7B28.)

23. Gillis, Clarence L., Polhamus, Edward C., and Gray, Joseph L., Jr.: Charts for Determining Jet-Boundary Corrections for Complete Models in 7- by 10-Foot Closed Rectangular Wind Tunnels. NACA WR L-123, 1945. (Formerly NACA ARR L5G31.)

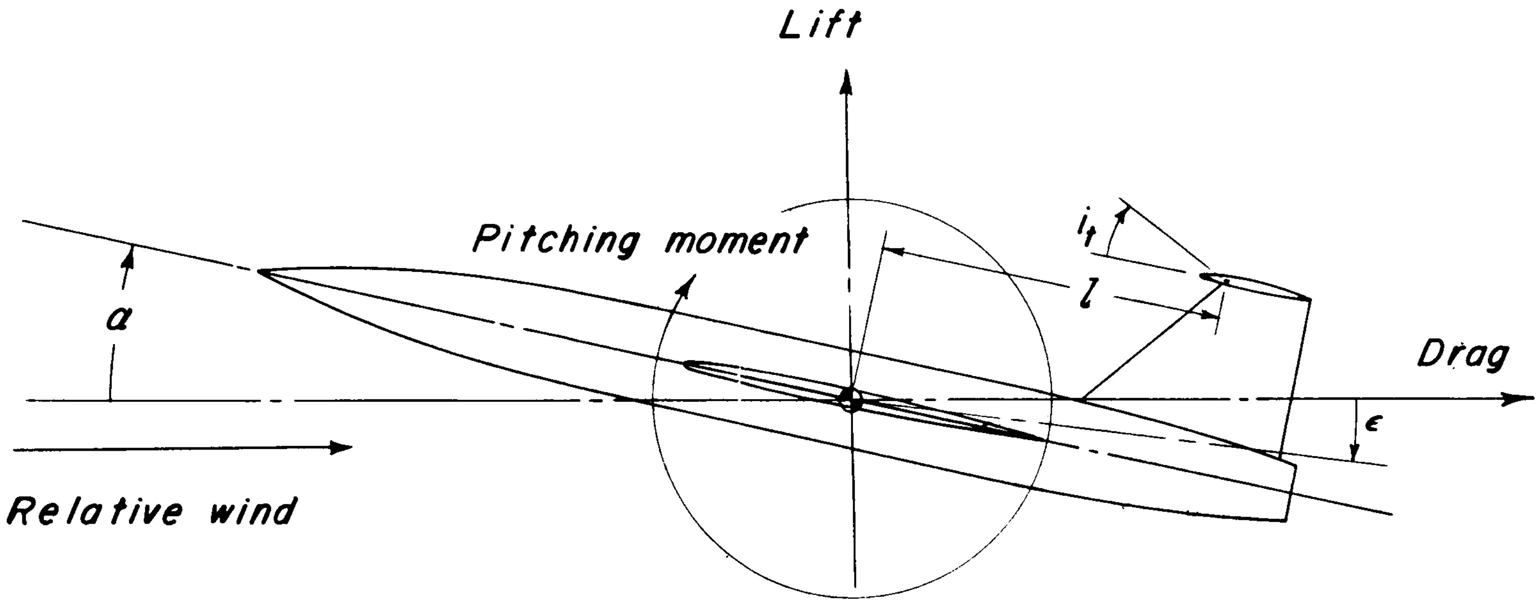

Figure 1.- Stability system of axes. Positive directions of forces, moments, and angles are indicated by arrows.

(1) Shortal- Maggin: (Ref. 4). Refers to moment-Break Near $C_{L,max}$. Applicable at low subsonic speeds. Taper ratio not considered.

(2) Furlong- McHugh: (Ref. 5). Considered taper ratio, curve shown is for $\lambda = 0$.

(3) Weil - Gray: (Ref. 6). Refers to Moment Break Near $C_{L,max}$. Applicable through Transonic Speeds. Taper ratio not considered.

(4) Few - Fournier: (Ref. 7). Refers to Moment Break at any Angle of Attack Through Transonic Speeds. Applicable to Highly Tapered Wings Only ($\lambda = 0$ to 0.4).

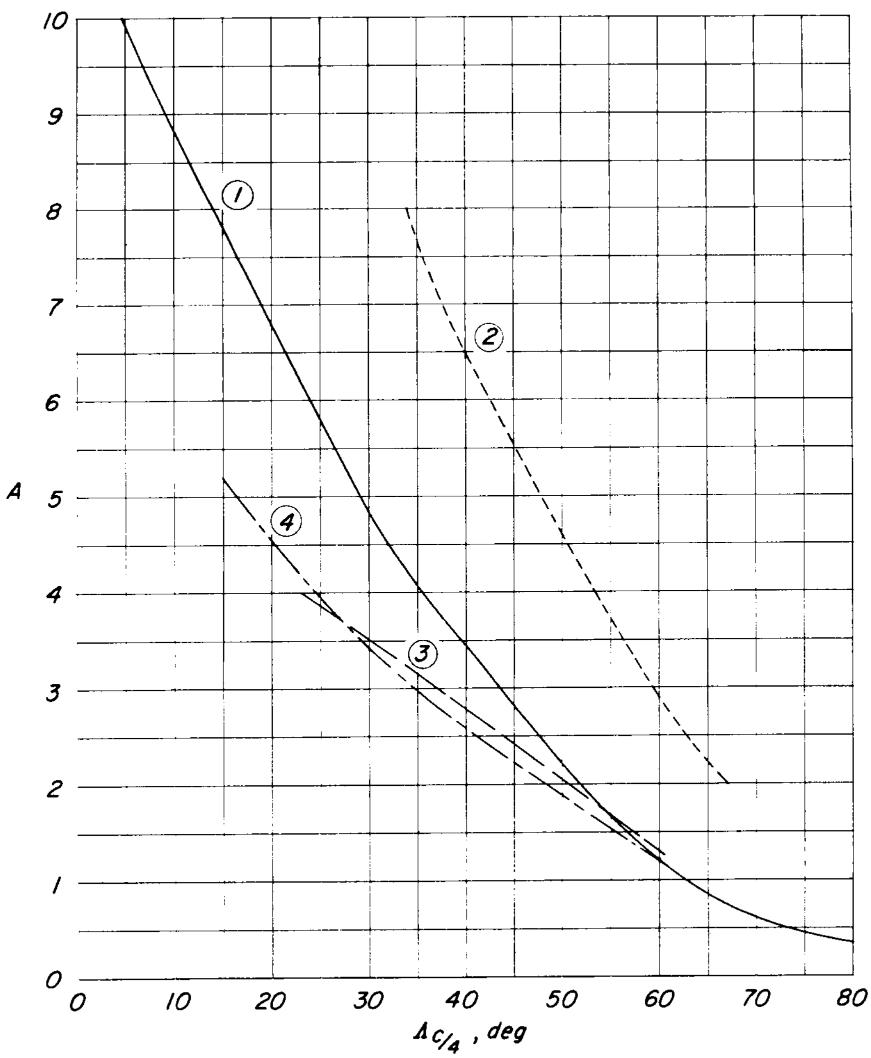

Figure 2.- Summary of boundaries that separate wings that are characterized by increased stability in the high lift range (area below and to left of curves) and wings with decreased stability in the high lift range (area above and to right of curves).

L-427

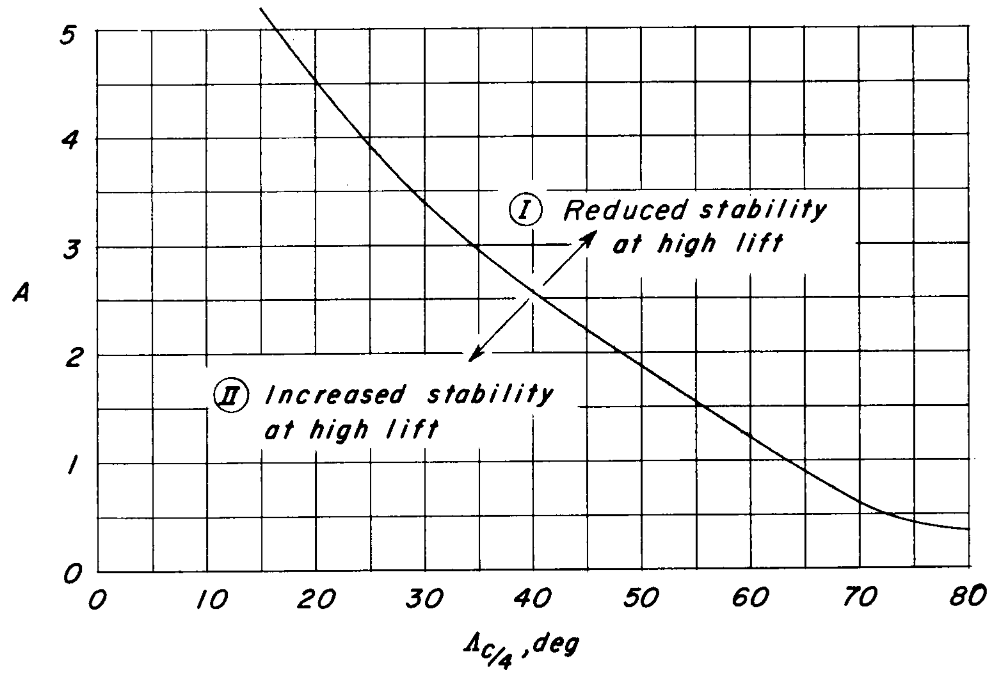

(a) Boundary related to wing plan form.

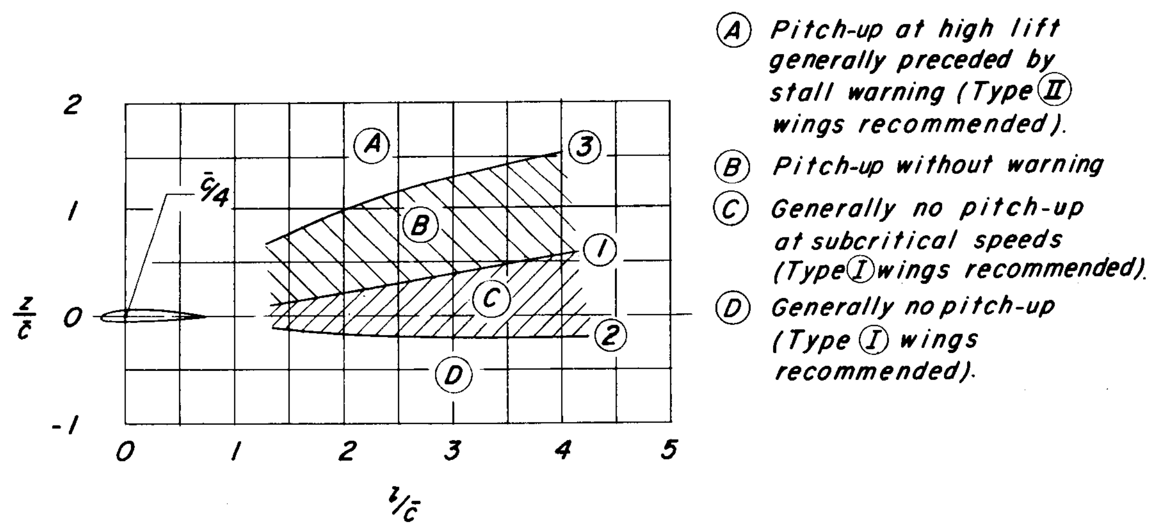

(b) Boundary related to horizontal-tail position.

Figure 3.- Approximate design guide for selection of wing plan forms and horizontal-tail position for achieving minimum pitching-moment nonlinearity. $\lambda = 0$ to 0.4.

L-427

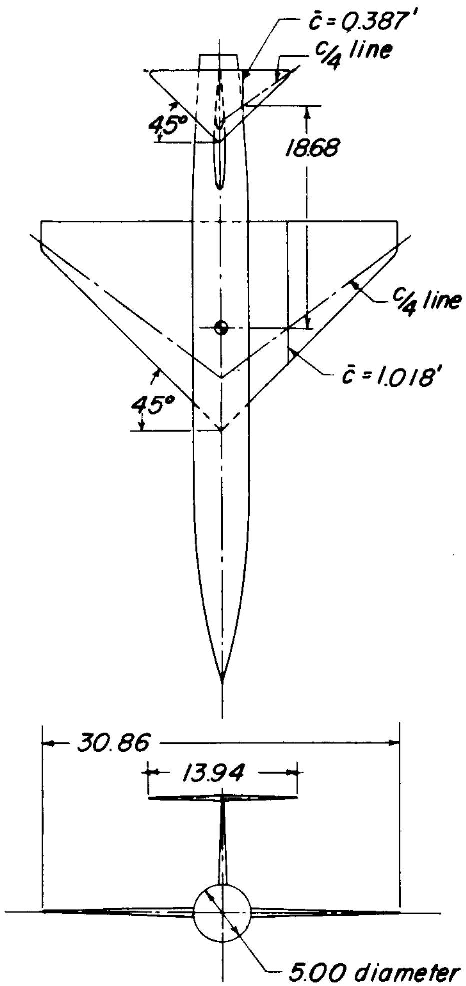

Geometric Characteristics of Test Model

	Wing	Horizontal tail	Vertical tail
Area, sq ft	2.20	0.337	0.603
A	3.00	4	1.16
λ	0.143	0	0.411
Tip chord, in.	2.57	0	5.04
Root chord, in.	18.00	6.97	12.27
$\Lambda_{c/4}$, deg	36.85	36.85	28.0
Airfoil section	NACA 65A006	NACA 65A006	NACA 65A006

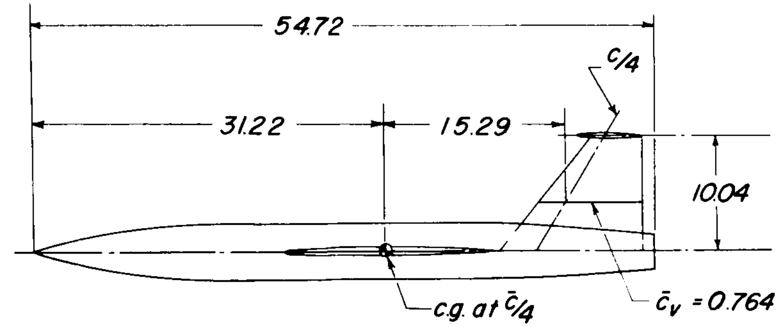

(a) Three-view drawing of aspect-ratio-3.0 model.

Figure 4.- Geometric characteristics of test models. All dimensions are in inches unless otherwise indicated.

L-427

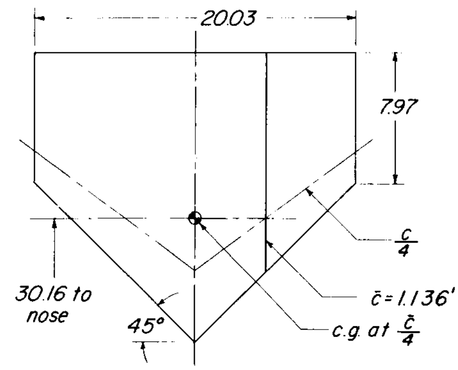

Aspect-ratio-1.55 wing

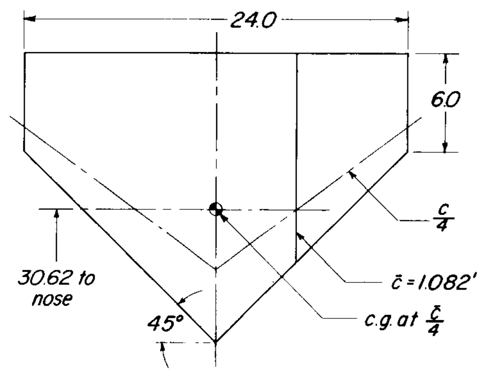

Aspect-ratio-2.0 wing

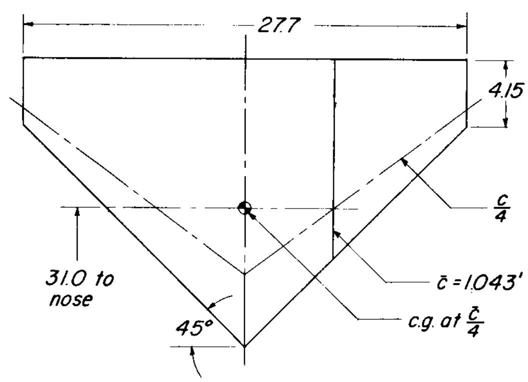

Aspect-ratio-2.5 wing

(b) Plan-form characteristics of three of the wings investigated.

Figure 4.- Concluded.

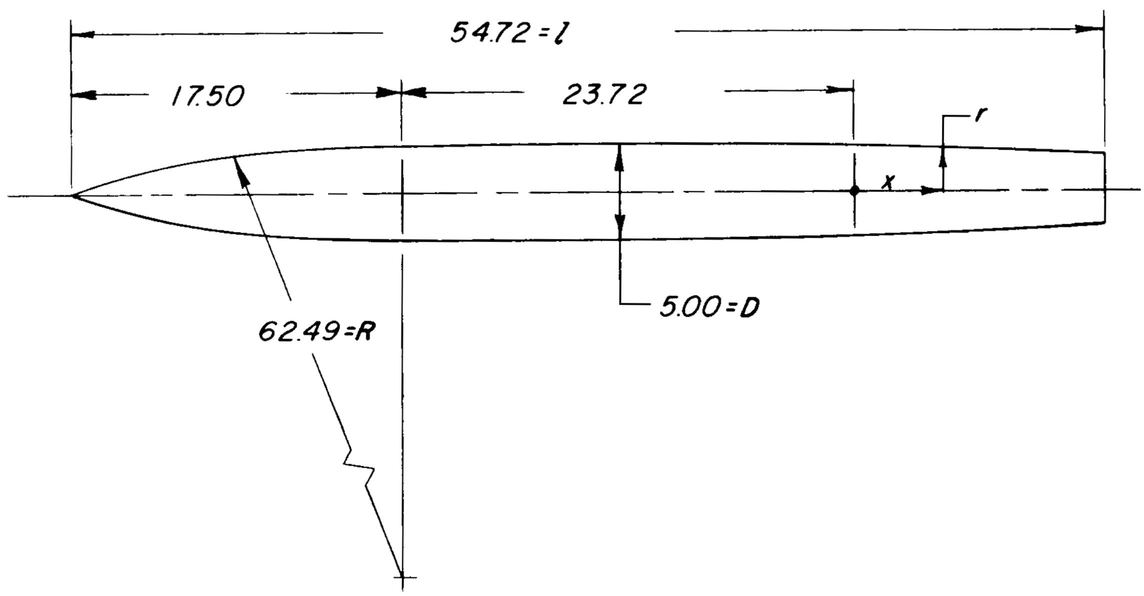

Afterbody Coordinates

x/l	r/l
0	.0456
.0320	.0445
.0639	.0427
.1187	.0390
Straight-line Taper	
.2460	.0301

Figure 5.- Details of fuselage. All dimensions are in inches.

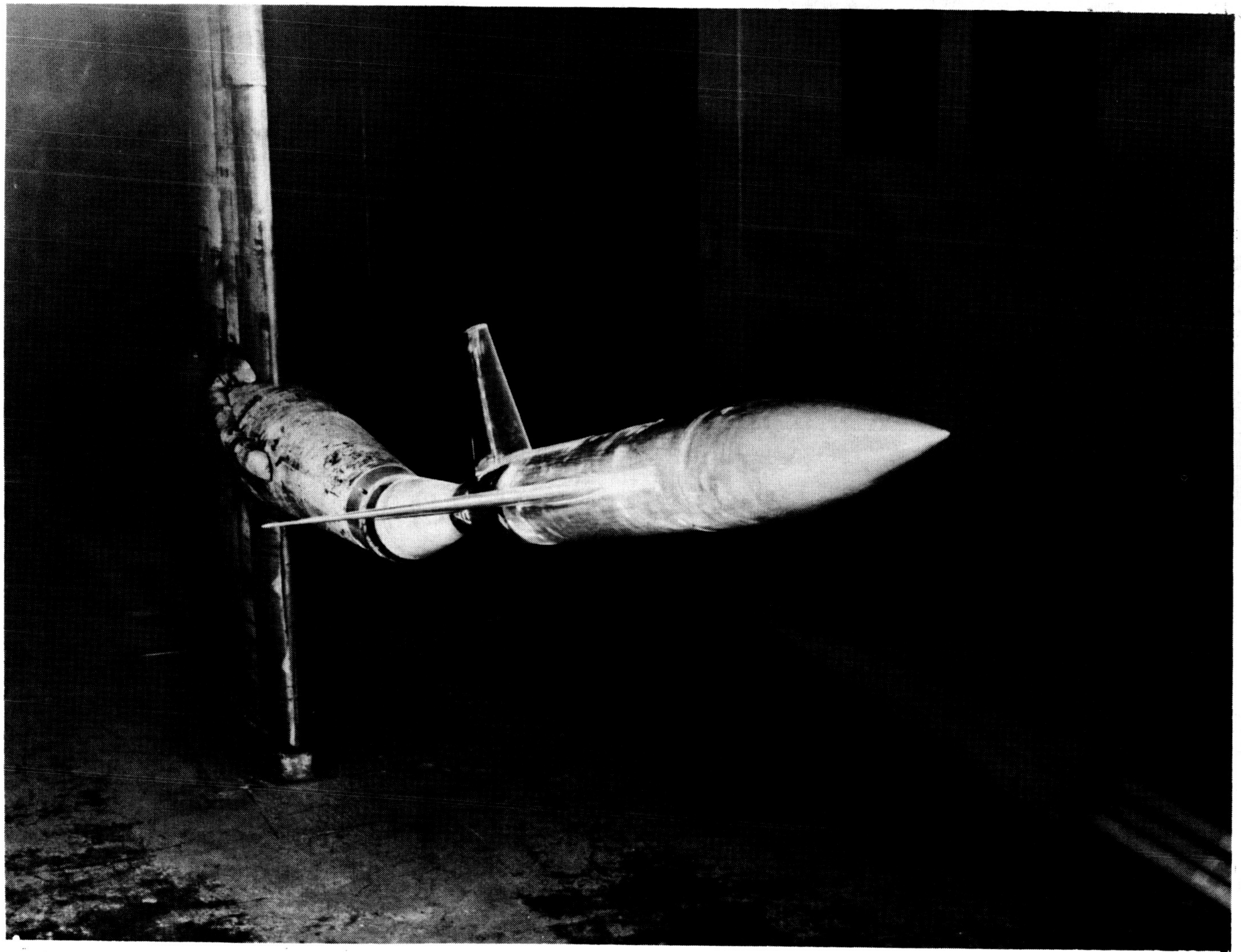

Figure 6.- Photograph of model mounted on tunnel sting support. L-83149

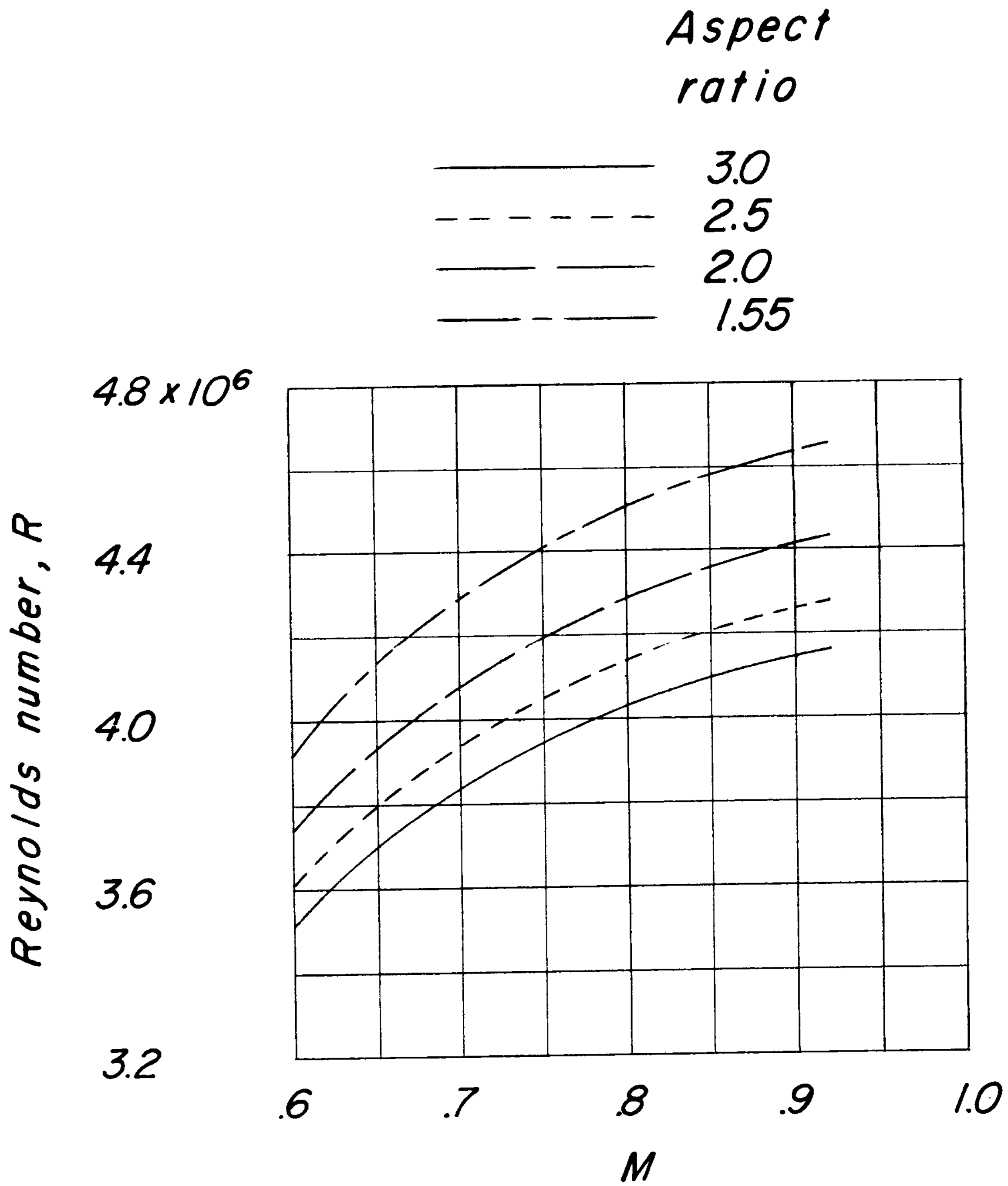

Figure 7.- Variation of mean test Reynolds number with Mach number for four wings investigated.

L-427

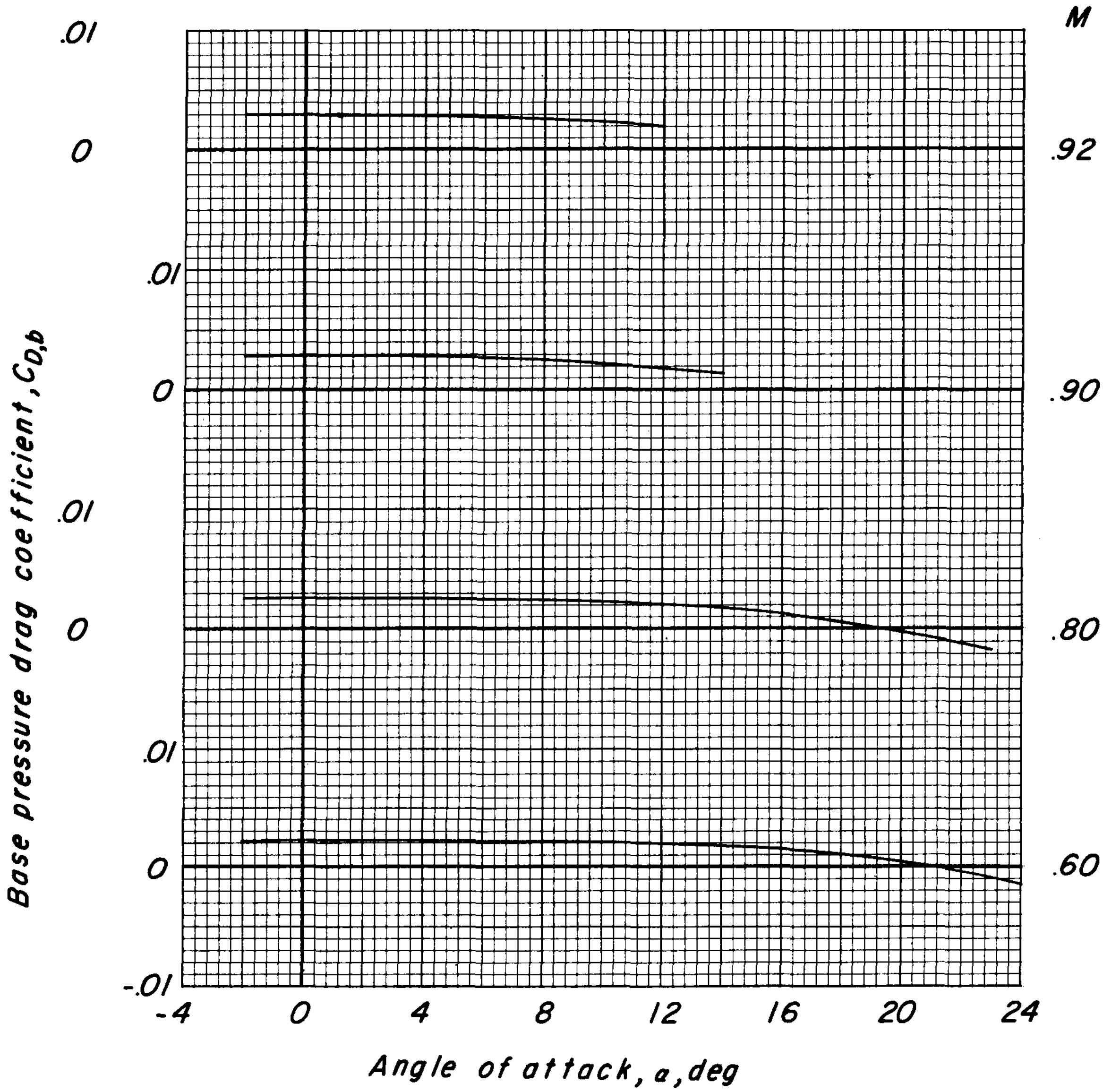

Figure 8.- Variation of base pressure drag coefficient with angle of attack and test Mach number. Based on aspect-ratio-3.0 wing.

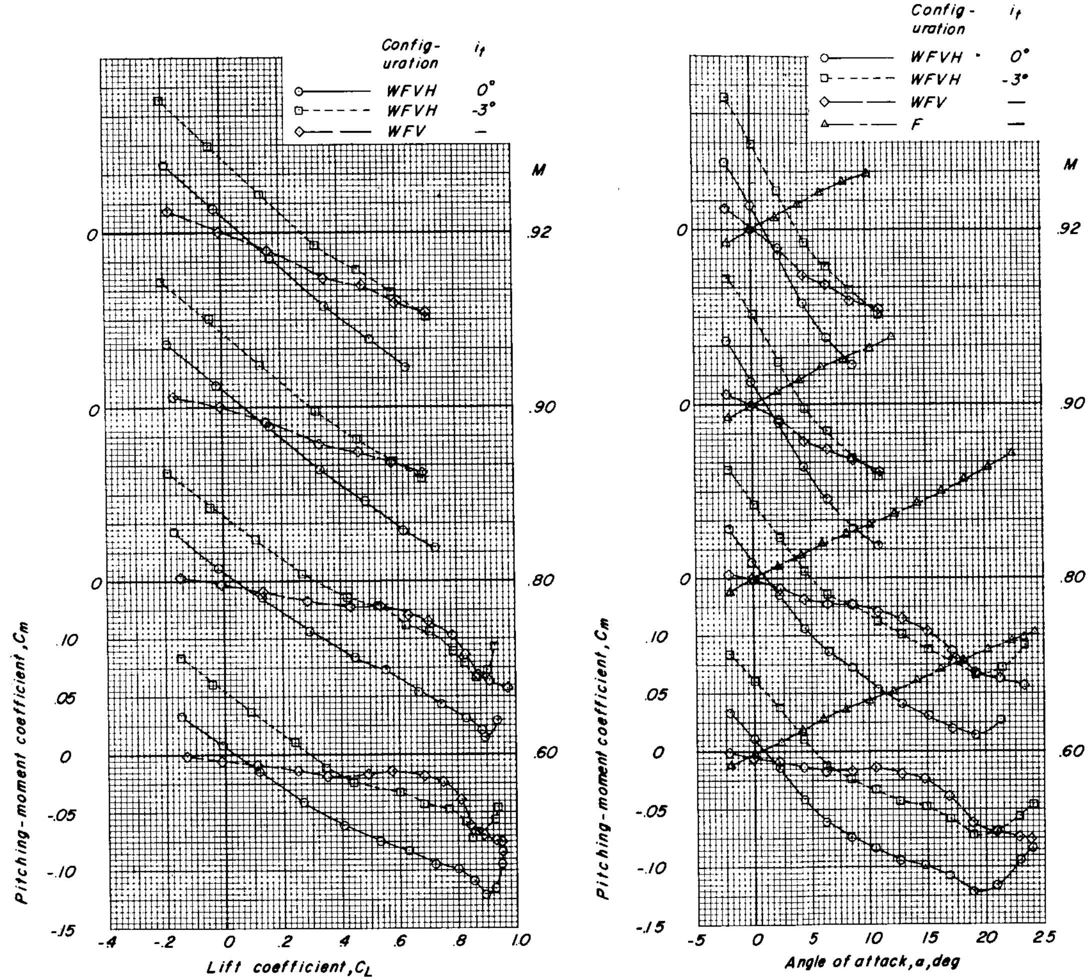

(a) Variation of C_m with C_L. (b) Variation of C_m with α.

Figure 9.- Aerodynamic characteristics of aspect-ratio-3.0 configuration showing effects of horizontal tail on and off and stabilizer deflection.

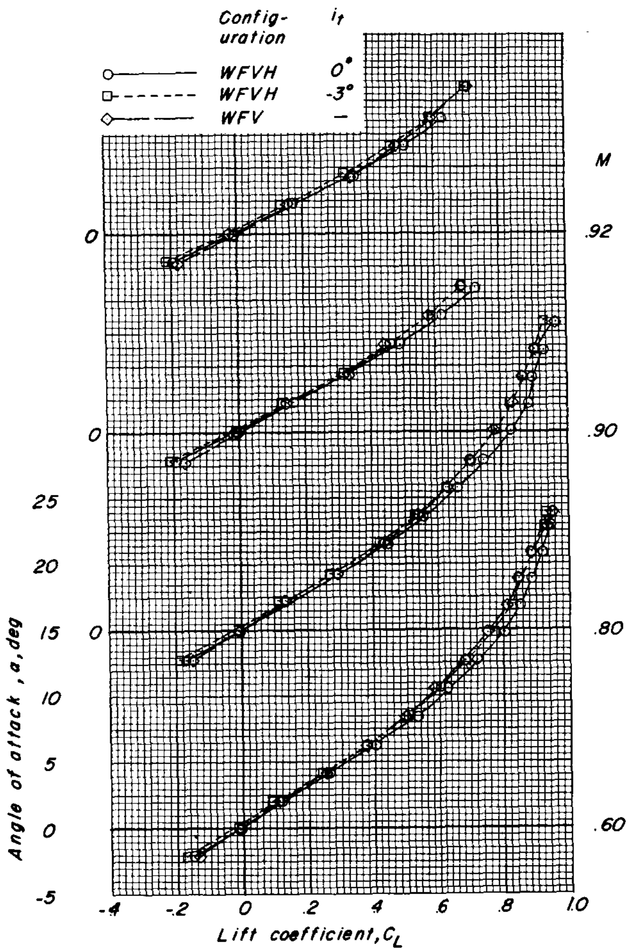

(c) Variation of α with C_L.

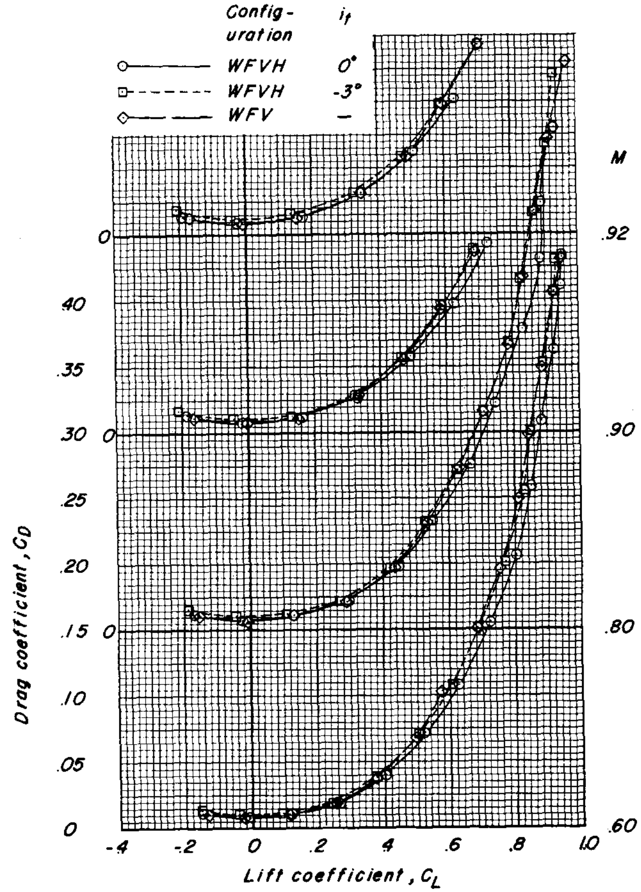

(d) Variation of C_D with C_L.

Figure 9.- Concluded.

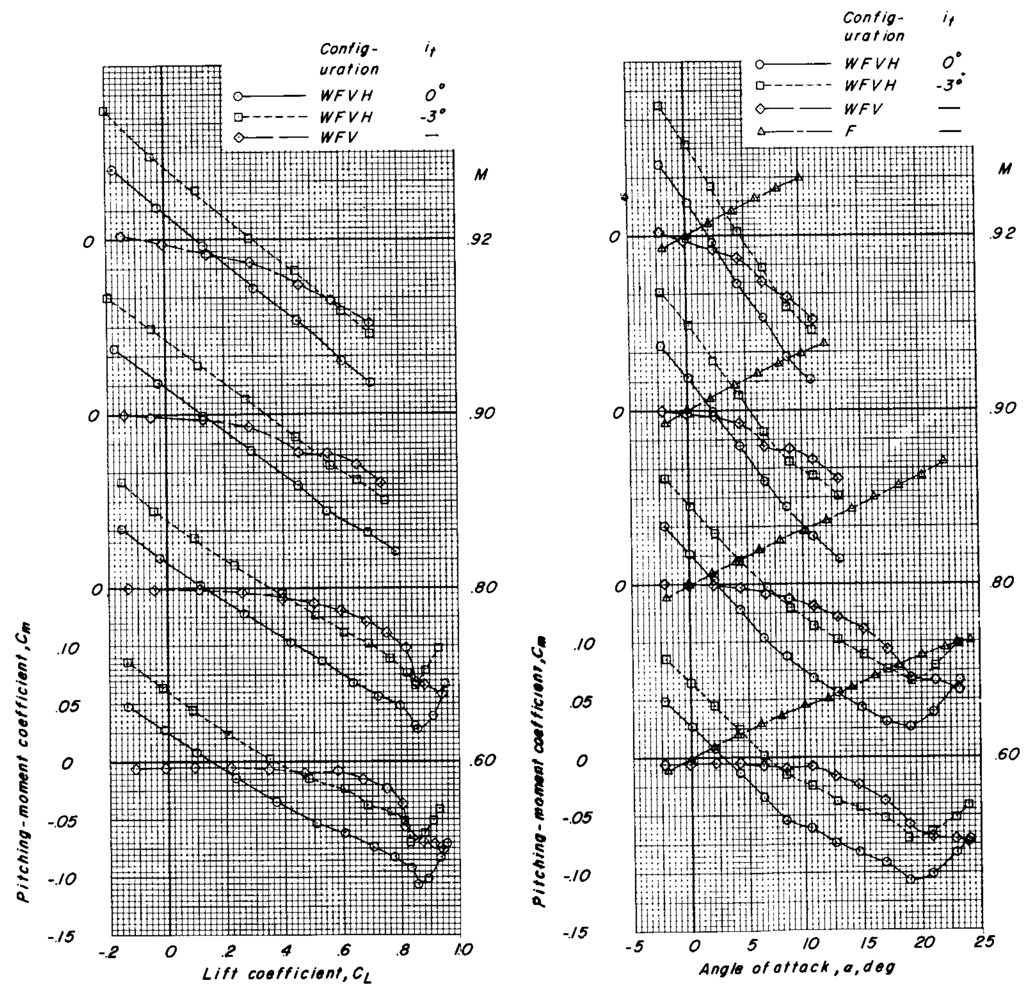

(a) Variation of C_m with C_L. (b) Variation of C_m with α.

Figure 10.- Aerodynamic characteristics of aspect-ratio-2.5 configuration showing effects of horizontal tail on and off and stabilizer deflection.

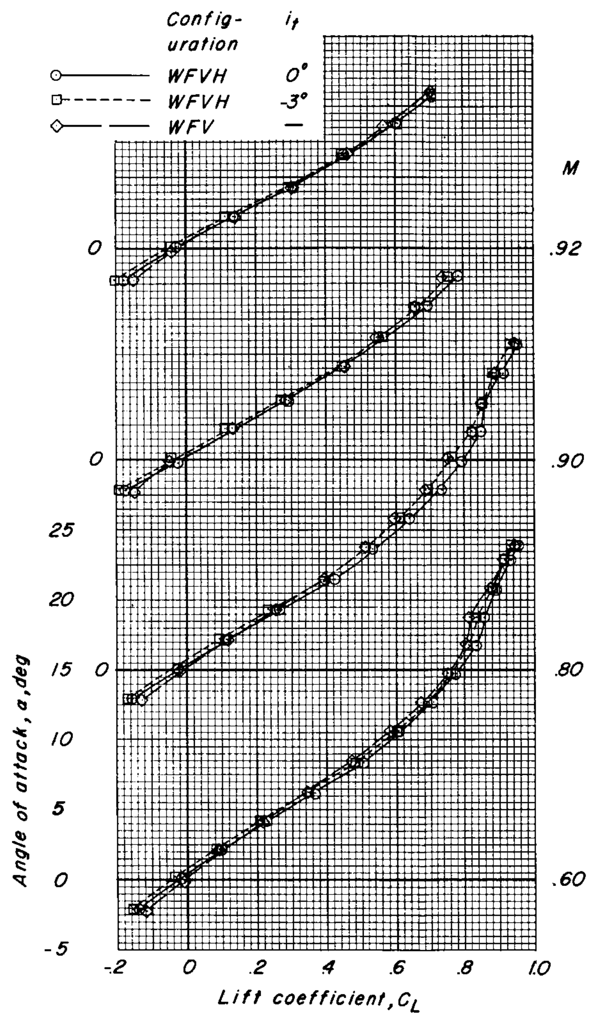

(c) Variation of α with C_L.

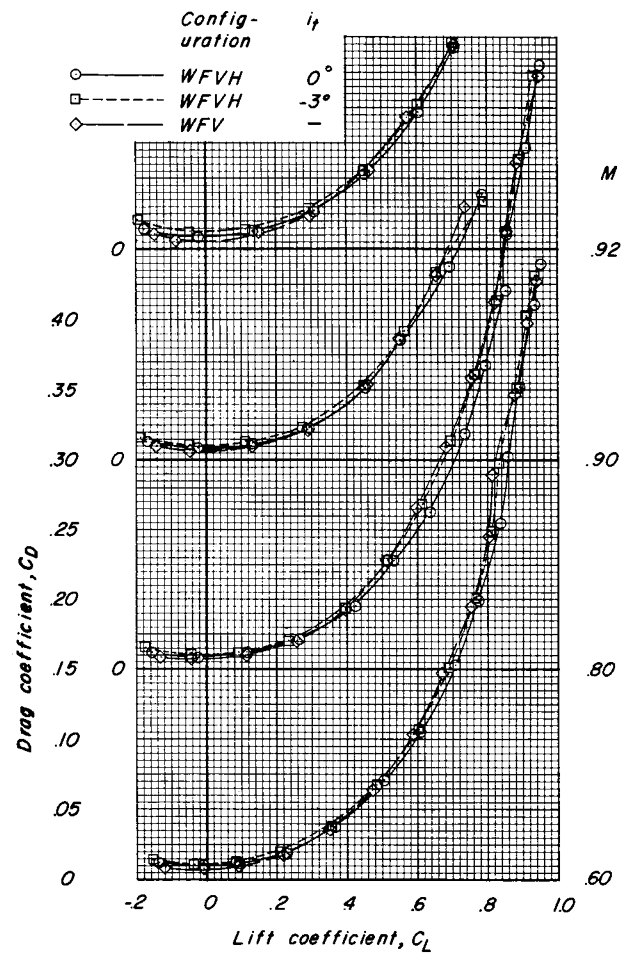

(d) Variation of C_D with C_L.

Figure 10.- Concluded.

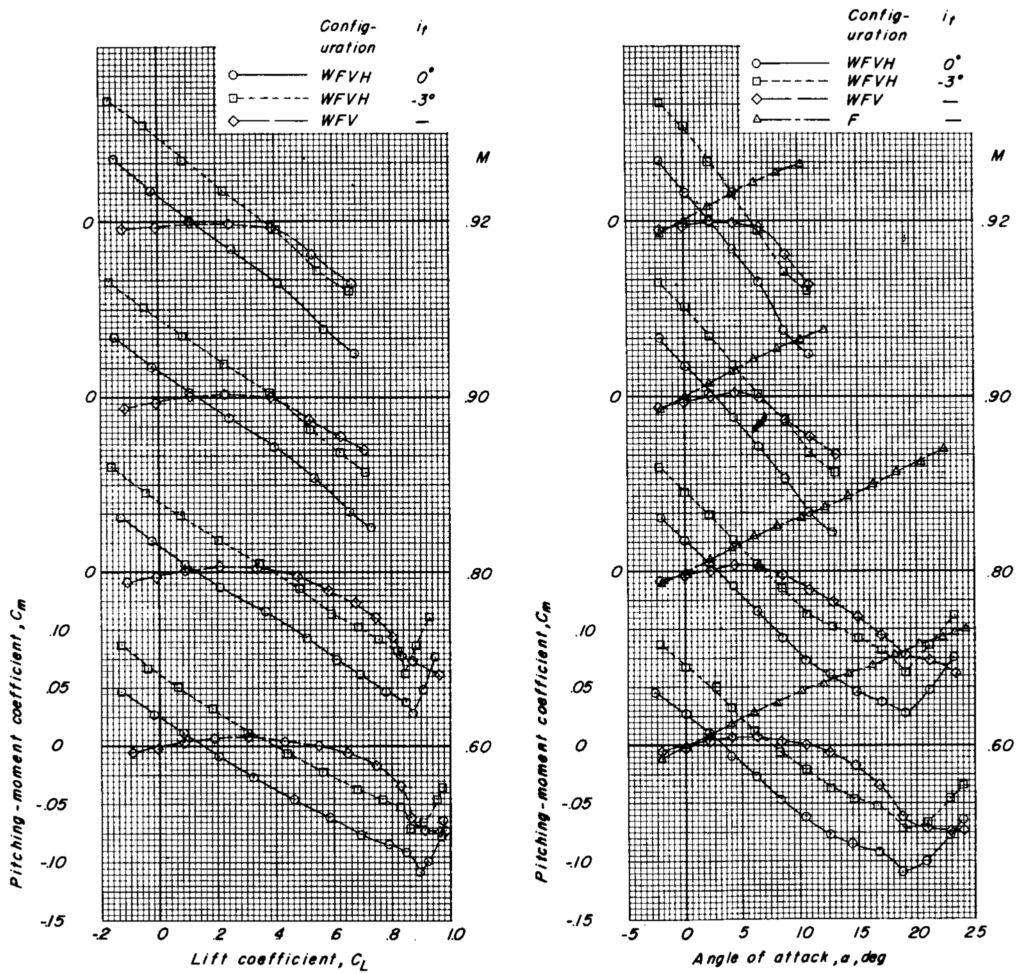

(a) Variation of C_m with C_L. (b) Variation of C_m with α.

Figure 11.- Aerodynamic characteristics of aspect-ratio-2.0 configuration showing effects of horizontal tail on and off and stabilizer deflection.

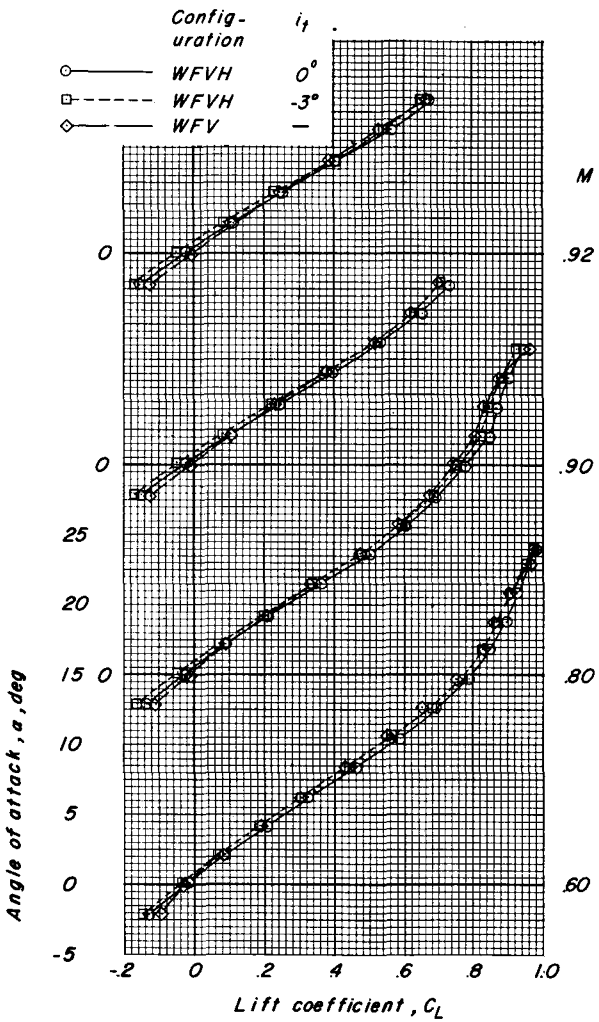

(c) Variation of α with C_L.

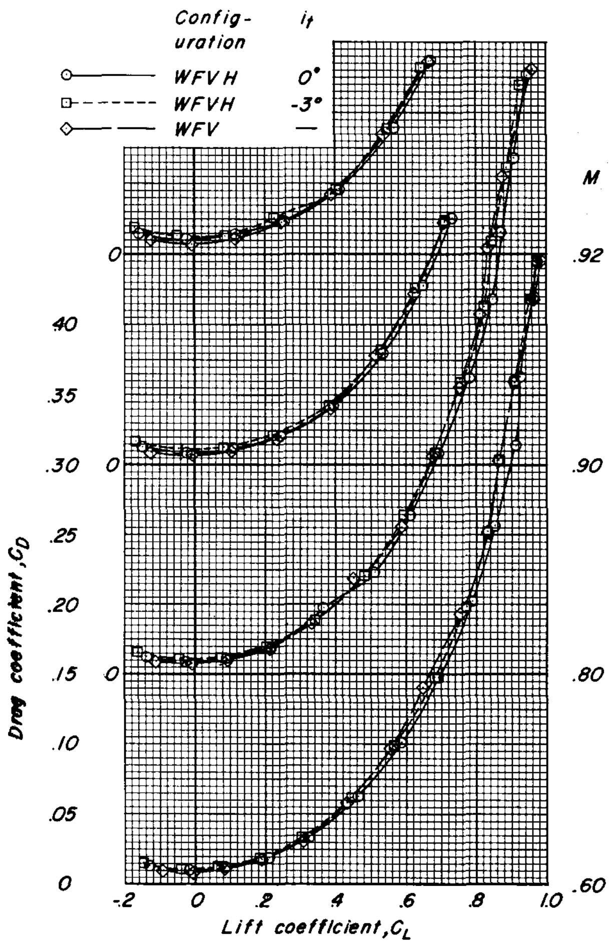

(d) Variation of C_D with C_L.

Figure 11.- Concluded.

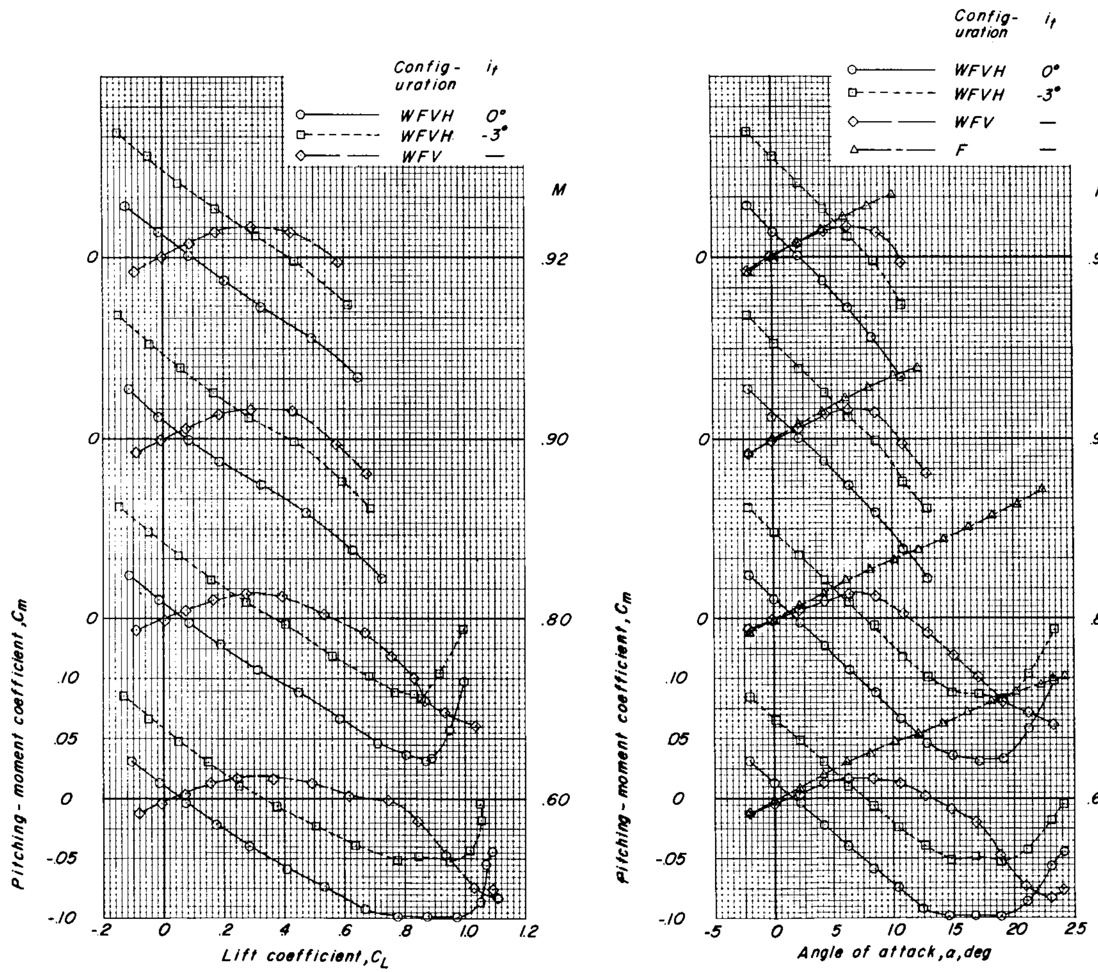

(a) Variation of C_m with C_L. (b) Variation of C_m with α.

Figure 12.- Aerodynamic characteristics of the aspect-ratio-1.55 configuration showing effects of horizontal tail on and off and stabilizer deflection.

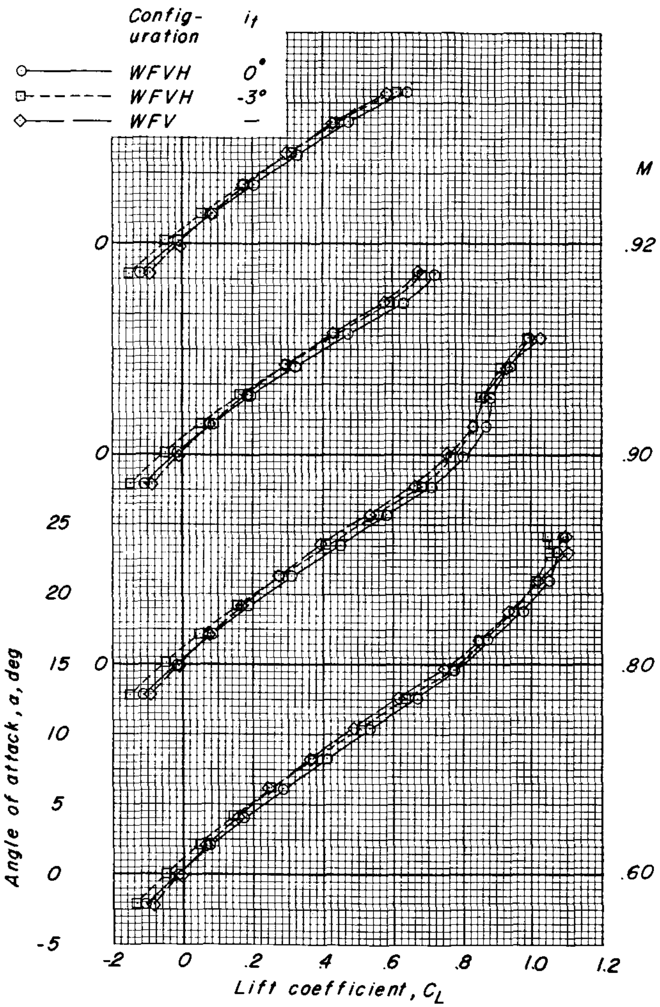

(c) Variation of α with C_L.

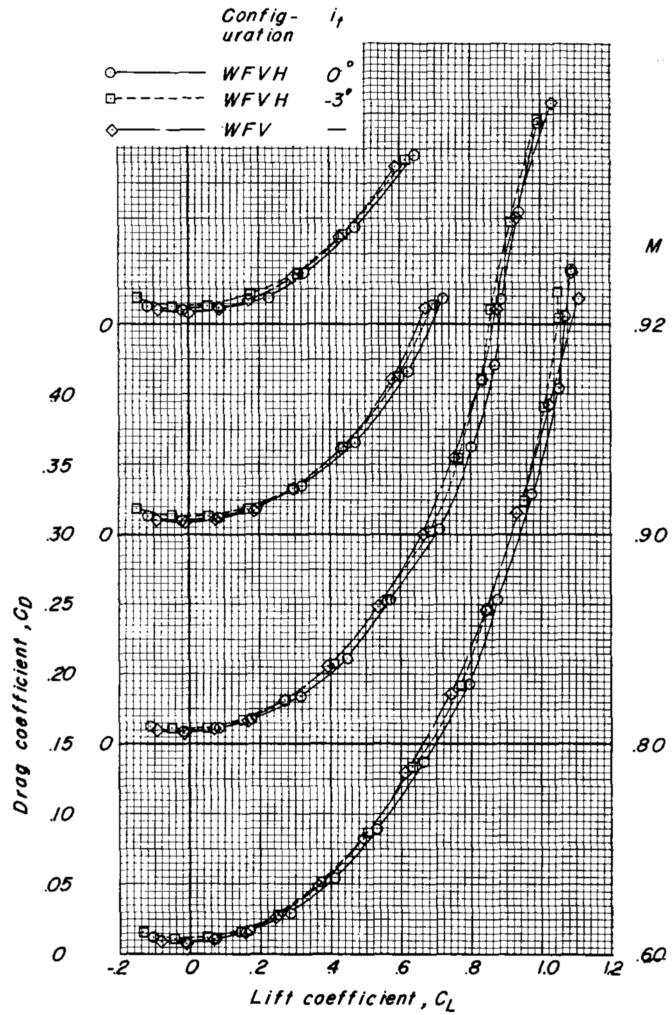

(d) Variation of C_D with

Figure 12.- Concluded.

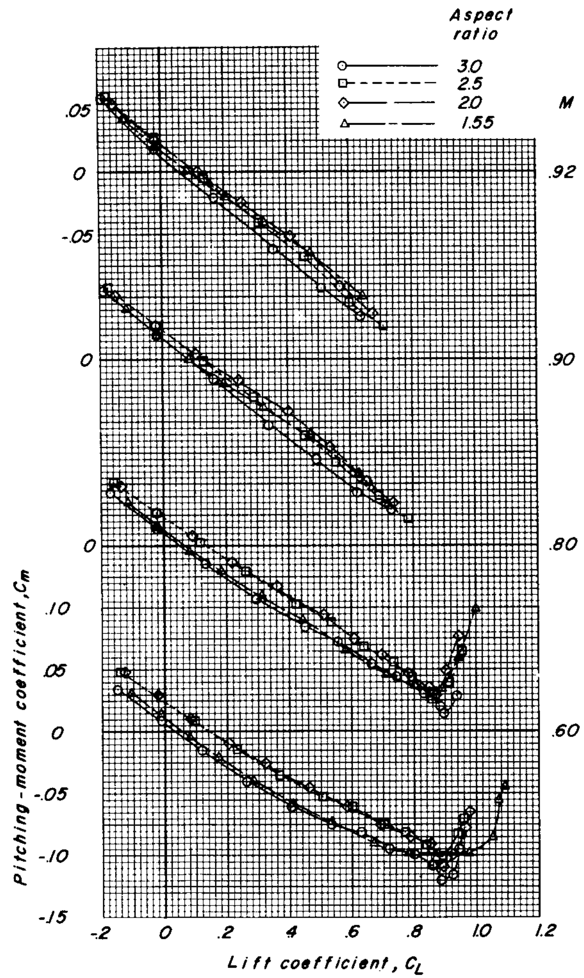

(a) Variation of C_m with C_L.

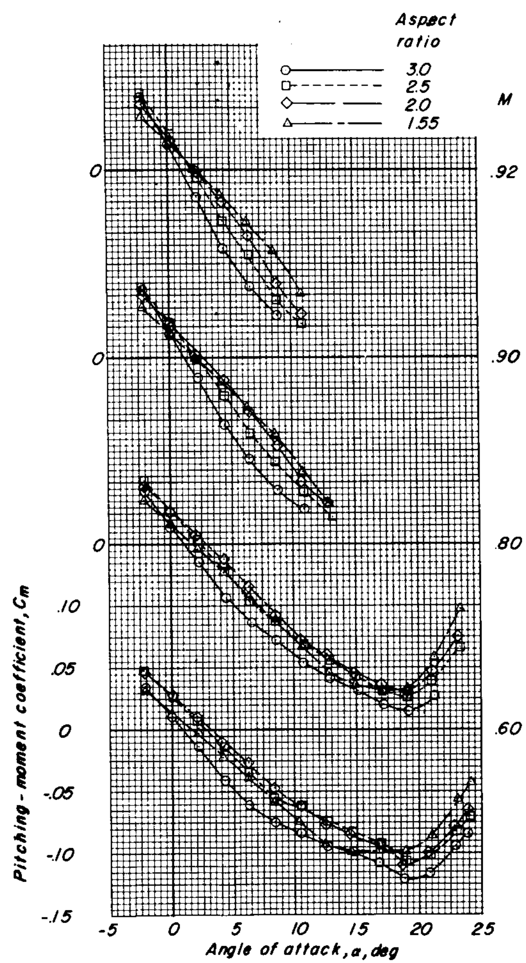

(b) Variation of C_m with α.

Figure 13.- Comparison of longitudinal aerodynamic characteristics of four configurations investigated. $i_t = 0^{\circ}$.

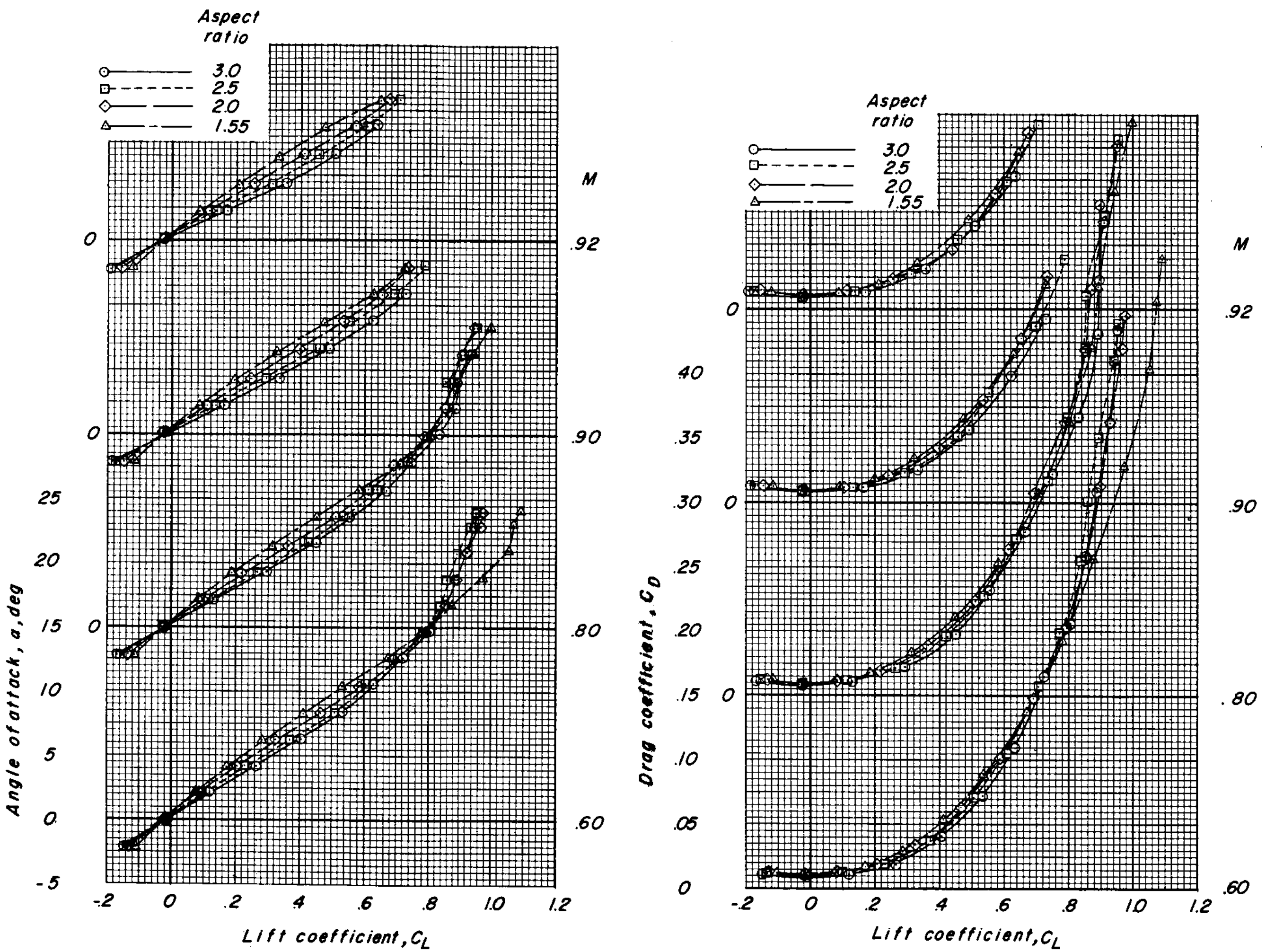

(c) Variation of α with C_L.

(d) Variation of C_D with C_L.

Figure 13.- Concluded.

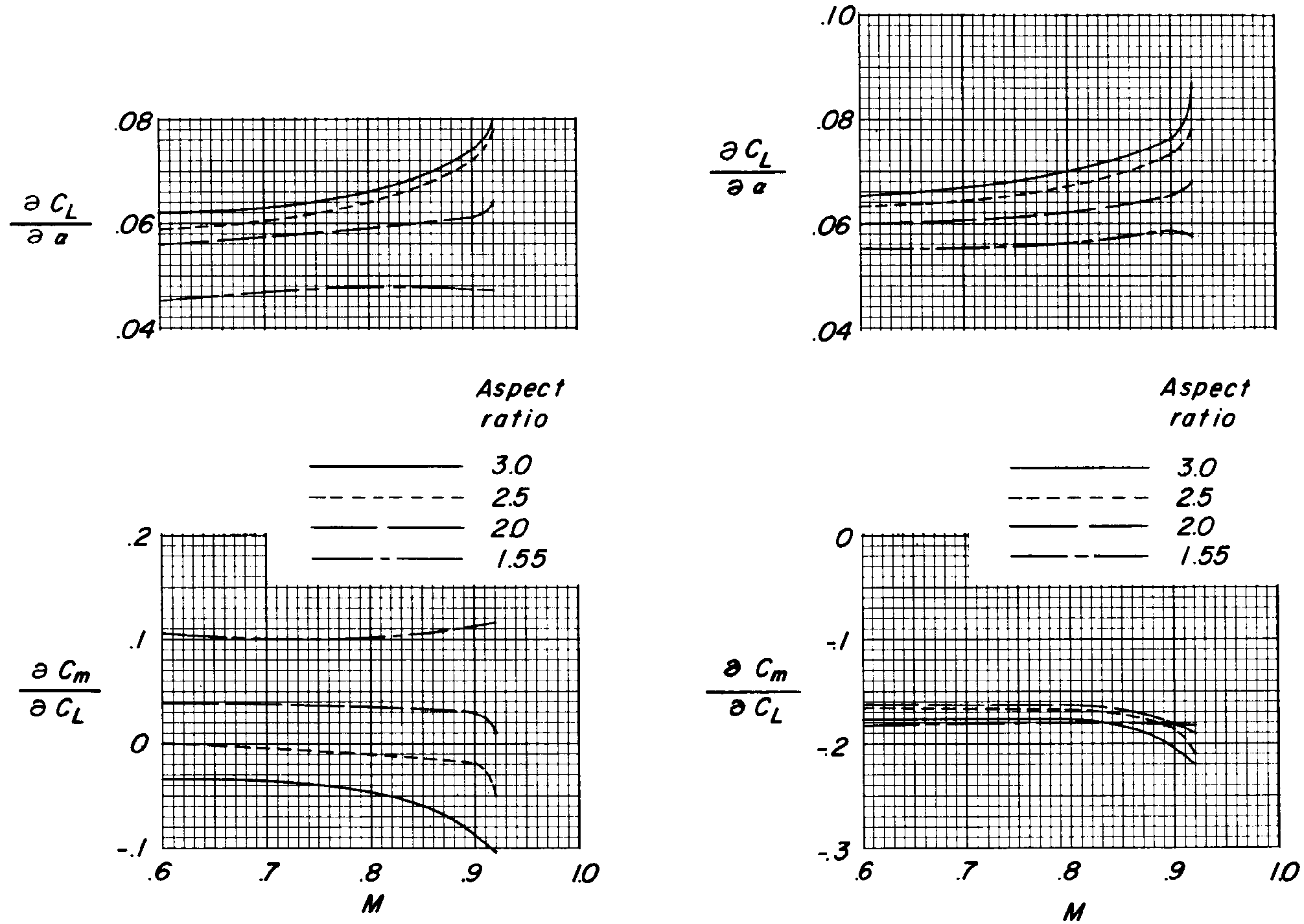

(a) Horizontal tail off. (b) Horizontal tail on. $i_t = 0^{\circ}$.

Figure 14.- Comparison of lift-curve slopes and static margin of stability of the four configurations investigated. Slopes taken between $C_L = 0$ to 0.3.

L-427

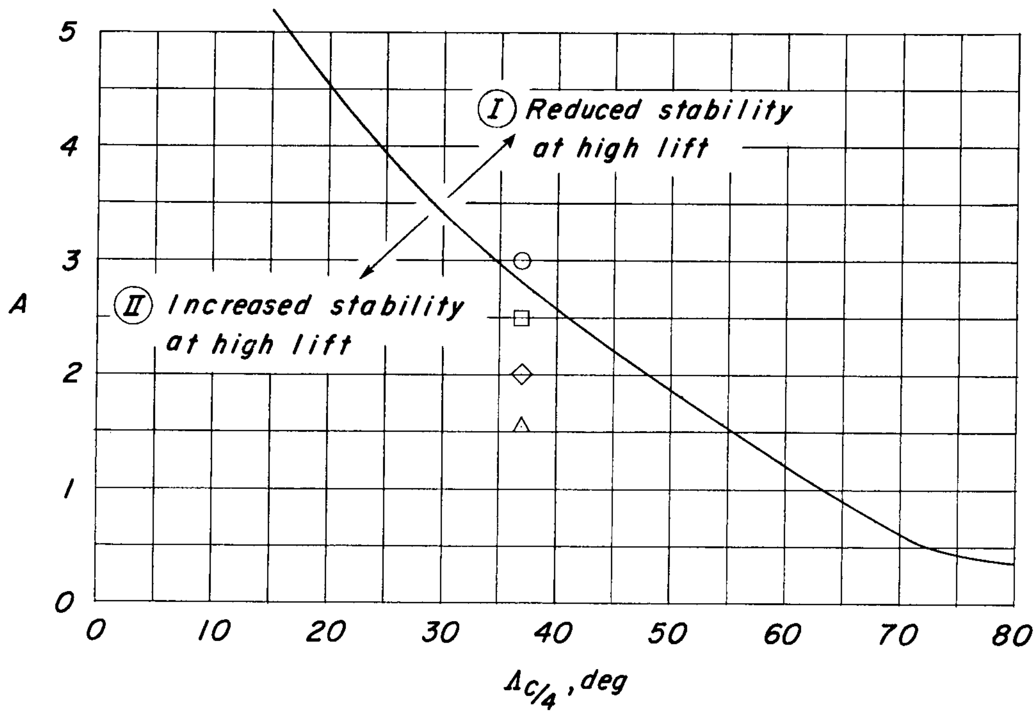

(a) Boundary related to wing plan form.

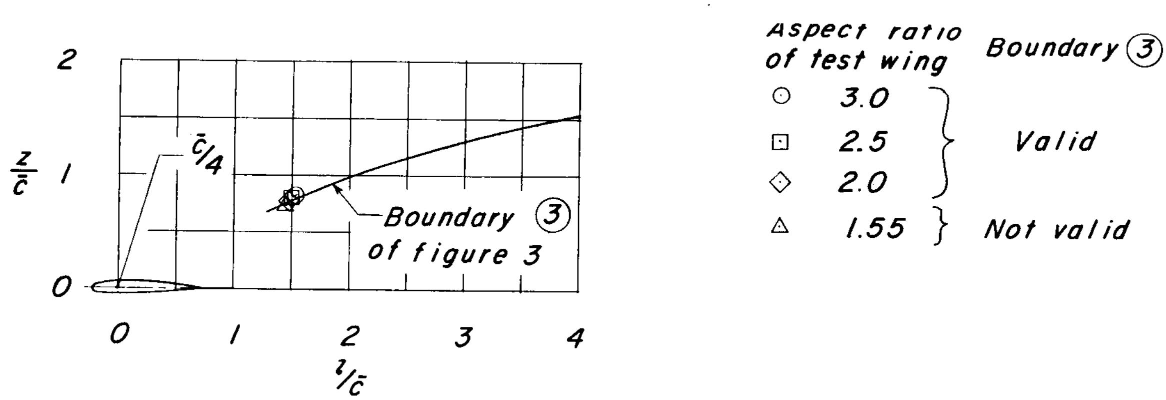

(b) Boundary related to horizontal-tail position.

Figure 15.- Comparison of geometric variables of test wings of this investigation with the approximate design guide of figure 3.